

Energetics of the summer circulation over South America

M. C. de Lima Moscati and V. Brahmananda Rao

Instituto Nacional de Pesquisas Espaciais/Ministério da Ciência e tecnologia - INPE/MCT 12.227-970 - São José dos Campos, SP - Brazil

Received: 21 December 1999 – Revised: 25 September 2000 – Accepted: 27 September 2000

Abstract. We have investigated the energetics of the summer circulation over tropical and extratropical South America. The kinetic energy equations of divergent (K_χ) and rotational (K_ψ) motion are utilized. All the terms of these equations are calculated on each day for five summers (November–February 1985–1990), using global wind analysis from the National Meteorological Center (NMC), now National Centers for Environmental Prediction (NCEP). The regional kinetic energy balance showed that the energy cycle over South America during the summer is, APE to K_χ through the term $-\chi \nabla^2 \Phi$, and K_χ to K_ψ through the term $f \nabla \psi \cdot \nabla \chi$. In the literature, several dominant oscillation modes have been noted over South America, namely the annual cycle, inter-annual, seasonal, intraseasonal, and high frequency scales, as revised by Lima. Results of the power spectrum analysis of kinetic energy terms indicate several statistically significant peaks and these have been confirmed with a fourth-order Butterworth filter. A well-defined mode, with a period around 30 days, was detected in the terms $-\chi \nabla^2 \Phi$ and $f \nabla \psi \cdot \nabla \chi$, likely associated with Madden-Julian Oscillation (MJO). Later, we discuss the local kinetic energy balance using Mak's local energetics scheme. We attempted to verify how the intraseasonal component interacts with other dominant oscillations over South America, such as seasonal cycle and high frequency disturbances. It is noted that the major interactions among the three temporal scales occur mainly close to the South Atlantic Convergence Zone (SACZ) region. The temporal scale interactions in the Bolivian High (BH) and Northeast Brazil Low (NL) are distinct, and the dominant temporal scales may change from year to year.

Key words. Meteorology and atmospheric dynamics (climatology, general circulation, tropical meteorology)

1 Introduction

Summer circulation over South America shows several interesting characteristics. In the upper troposphere a warm

anticyclone, known as the Bolivian High (BH) develops over the Bolivian-Peruvian altiplano during the austral summer. To the east of this high in the upper levels a trough forms extending to the western South Atlantic. This is known as the Northeast Brazil Low (NL). At low levels a continental low develops in the region of Paraguayan-Argentinian Gran Chaco and Papeau Sierras. Northerly and northwesterly low-level flow is seen along the eastern slopes of the tropical and subtropical Andes while east-northeasterly trades prevail over much of the Amazon basin. These low-level winds are important for the moisture flux and rainfall over South America during the summer (Rao et al., 1996). Virji (1981) deduced most of the characteristics of the summer circulation over South America using early observations of the cloud wind data obtained from geostationary satellites. Figueroa and Nobre (1990) studied the structure of the climatological summer rainfall over South America and the mechanisms associated with them.

There are two suggestions for the origin of the Bolivian High. Gutman and Schwerdtfeger (1965) suggested that it is maintained by the heat source mainly, the latent heat over the plateau. Rao and Erdogan (1989) confirmed the importance of latent heating. Another interesting aspect of Rao and Erdogan's (1989) study is the comparison of the intensity of heat source over the Altiplano in South America and eastern Tibet. They found that heating over northeastern Altiplano was stronger in 1979 than that over eastern Tibet. The Tibetan High in the upper troposphere is a part of the well-known summer monsoon circulation over South Asia. On the other hand, studies by Silva Dias et al. (1983), DeMaria (1985), Kleeman (1989), Gandu and Geisler (1991), Figueroa et al. (1995) and others, suggest the importance of Amazonian heating instead of heating over the Altiplano for the formation of the Bolivian High. Recently Lenters and Cook (1997) examined the characteristics of upper tropospheric summer circulation over South America using a general circulation model, a linear model and observational data. They noted that the BH and accompanying NL are generated in response to precipitation over the Amazon basin, central Andes and South Atlantic Convergence Zone (SACZ) with African precipitation also playing a crucial role in the gener-

ation of NL. Regarding the position of BH, Lenters and Cook (1997) concluded that it is primarily determined by Amazonian precipitation.

In a recent study Chen et al. (1999) discussed the maintenance of austral summertime upper tropospheric circulation over tropical South America, in particular the BH–NL system. They discussed the spatial relationship between the velocity potential (χ) and stream function (ψ) and suggested that the BH–NL system is maintained by South American local heating and remote African heating. They pointed out the existence of the Sverdrup balance for the BH–NL system which agrees with a similar conclusion reached by Lenters and Cook (1997).

Although the general aspects of the atmospheric circulation over South America have become better known in recent years, their dynamics have not yet been completely understood. Thus, we propose to investigate the energetics of the summer circulation over South America by separating the kinetic energy into the ψ and χ parts. We use the formalism of Krishnamurti and Ramanathan (1982) and Krishnamurti et al. (1998) to estimate the generation of kinetic energy and to determine the energy cycle for this region. This will help to understand how kinetic energy in ψ and χ parts is maintained. We calculated the energy conversion terms on a daily basis for the summer season (November–February 1985–1990) and, in addition, we intend to detect the dominant oscillation modes. We also study the local energetics using the methodology developed by Mak (1991), which separates the kinetic energy (K) into seasonal, intraseasonal and high frequency components, attempting to analyze what are the dominant periodicities in the daily values of K_ψ and K_χ , and how these oscillations are maintained.

Section 2 presents the data and methodology. Section 3 describes the results and discussions, where the regional energetics (Sect. 3.1), periodicities in the energetics (Sect. 3.2) and local energetics (Sect. 3.3) are discussed. There follows a brief section of concluding remarks.

2 Data and methodology

We have used global data set obtained from NMC (National Meteorological Center, now National Centers for Environmental Prediction NCEP). The variables used are zonal wind (u), meridional wind (v), geopotential height (z) and temperature (T) fields with a rhomboidally truncated 30 wave number (R30) at 12 UTC. There were 12 pressure levels between 1000 hPa each at 50 hPa. The original data are available from 1 November 1985 to 31 January 1991. When the present work was performed the NCEP reanalysis data were not available to us.

Some modifications were made in the operational model of the NMC during the period from 1985 to 1988 (Trenberth and Olson, 1988). The changes in the analytical procedures and their influence on the data are described by Trenberth and Olson (1988), Mo and Rasmusson (1993), and Kanamitsu and Saha (1995). Here, emphasis will be given to the sum-

mer season (November to February – NDJF). Trenberth and Olson (1988) compared the European Center for Medium Range Weather Forecasts (ECMWF) and NMC data. They found that NMC data show major problems prior to May 1986 south of 50°S. In general the representation of divergent wind improved as the analytical procedures became more sophisticated to include more realistic diabatic heating effects. This introduced discontinuities. In general, the data over continents (including South America) should be considered superior compared with those over the Southern Oceans. Mo and Rasmusson (1993) found that the overall agreement in the vorticity balance at 200 hPa between NMC and ECMWF was generally satisfactory. Kanamitsu and Saha (1995) evaluated the systemic errors in NMC analysis and this will be discussed later while analyzing the kinetic energy budget over South America.

The divergence (D), the vorticity (ζ), χ , ψ and the divergent horizontal wind (u_χ , v_χ) and rotational horizontal wind (u_ψ , v_ψ) components were calculated from the global spectral components. These fields were transformed to a global grid (96×76 points), which corresponds to 3.75° longitude by about 2.25° latitude on the transformed grid. The kinematic method was used for computing vertical motion, considering for the lower and upper boundary conditions (at level 1000 hPa and 50 hPa, respectively) a value of zero for ω . A linear mass adjustment in divergence field is made to reduce inherent observational errors (Lima, 1996). With these data at grid points the energy parameters were calculated.

Here we use the Krishnamurti and Ramanathan (1982) and Krishnamurti et al. (1998) budget equations for K_ψ and K_χ , expressed by the relations:

$$\left\langle \left\langle \frac{\partial K_\psi}{\partial t} \right\rangle \right\rangle = \langle \langle B_\psi \rangle \rangle + \langle \langle C(K_\chi, K_\psi) \rangle \rangle - \langle \langle D(K_\psi) \rangle \rangle \quad (1)$$

$$\left\langle \left\langle \frac{\partial K_\chi}{\partial t} \right\rangle \right\rangle = \langle \langle B_\chi \rangle \rangle + \langle \langle C(APE, K_\chi) \rangle \rangle - \langle \langle C(K_\chi, K_\psi) \rangle \rangle - \langle \langle D(K_\chi) \rangle \rangle \quad (2)$$

In these equations APE denotes available potential energy, B_ψ and B_χ denote boundary flux terms, and D_ψ and D_χ denote dissipations terms, which we ignore in this study. The energy conversion terms are represented by the bracketed terms, the positive sign denotes an energy exchange from the first to the second member. The double brackets $\langle \langle \cdot \rangle \rangle$ denote the integrations in the horizontal and vertical domain.

The various components of the budget equations are defined by relations:

$$\langle \langle C(APE, K_\chi) \rangle \rangle = \left\langle \left\langle -\chi \nabla^2 \Phi \right\rangle \right\rangle \quad (3)$$

$$\begin{aligned} \langle \langle C(K_\chi, K_\psi) \rangle \rangle &= \langle \langle f \nabla \psi \cdot \nabla \chi \rangle \rangle + \left\langle \left\langle \nabla^2 \psi \nabla \psi \cdot \nabla \chi \right\rangle \right\rangle \\ &+ \left\langle \left\langle \nabla^2 \chi \frac{((\nabla \psi)^2)}{2} \right\rangle \right\rangle + \left\langle \left\langle \omega J \left(\psi, \frac{\partial \chi}{\partial p} \right) \right\rangle \right\rangle \end{aligned} \quad (4)$$

$$\langle \langle K_\psi \rangle \rangle = \frac{1}{2} \left\langle \left\langle (u_\psi^2 + v_\psi^2) \right\rangle \right\rangle \quad (5)$$

$$\langle\langle K_\chi \rangle\rangle = \frac{1}{2} \langle\langle (u_\chi^2 + v_\chi^2) \rangle\rangle \quad (6)$$

the expressions (3) and (4) represent the generation of K (if $\langle\langle C(APE, K_\chi) \rangle\rangle > 0$) and interactions between K_ψ and K_χ , respectively. J represents the Jacobian operator and ∇^2 is the two-dimensional spherical Laplace operator. Other terms are already defined earlier. The interpretation of each term in the budget Eqs. (1 and 2) was made by Krishnamurti and Ramanathan (1982).

The magnitude of the term $f\nabla\psi \cdot \nabla\chi$ depends on the orientation of the vectors $\nabla\psi$ and $\nabla\chi$. In the Southern Hemisphere, if $\nabla\psi \cdot \nabla\chi < 0$ the energy exchange is from K_χ to K_ψ , while it is opposite if $\nabla\psi \cdot \nabla\chi > 0$. If $\nabla\psi$ and $\nabla\chi$ are perpendicular, no energy exchange occurs between these components.

The term $\nabla^2\psi(\nabla\psi \cdot \nabla\chi)$ expresses the vorticity effect on kinetic energy budget of K_χ and K_ψ components, since $\zeta = \nabla^2\psi$. It is important near the equator where f is small. The magnitude of this term also depends on the orientation of vectors $\nabla\psi$ and $\nabla\chi$.

The term $\nabla^2\chi(\nabla\psi)^2/2$ depends on covariance of the horizontal divergence $\nabla \cdot \mathbf{V}_H = -\nabla^2\chi$ and the kinetic energy of the nondivergent component $K_\psi = (\nabla\psi \cdot \nabla\psi)/2$. At any point the contribution of this term to K_ψ can be written as $\partial K_\psi/\partial t = \nabla^2\chi(K_\psi)$ or $\partial/\partial t \log K_\psi = \nabla^2\chi$. Thus, this term leads to exponential growth of K_ψ wherever $\nabla^2\chi$ is positive.

The term $\omega J(\psi, \partial\chi/\partial p)$ expresses the role of vertical motion in kinetic energy change, since $\partial\chi/\partial p \cong -\lambda^2\partial/\partial p\nabla^2\chi$ and the λ^2 is the Rossby deformation ratio. A simple interpretation of this term is difficult.

The term $-\chi\nabla^2\Phi$ represents the role of vertical circulations (Hadley and east-west) in the APE liberation, associated with warm (cold) air rising and cold (warm) air sinking in the domain.

Order of magnitude calculations show that the first two terms in Eq.(4) depend on the orientation of $\nabla\psi$ and $\nabla\chi$. Furthermore, these terms oppose each other and $f\nabla\psi \cdot \nabla\chi$ is the largest term (Chen and Wiin-Nielsen, 1976; Krishnamurti and Ramanathan, 1982; and others).

Also the zonal kinetic energy (\bar{K}) is calculated in the two areas of interest (see below), expressed by $\langle\langle \bar{K} \rangle\rangle = \langle\langle \bar{u}^2/2 \rangle\rangle$.

For the analysis of periodicities in the energy terms of the budget equations we build a time series for each energy parameter, calculating day-by-day, for each summer at each grid point, \bar{K} , K_χ and K_ψ terms at level 200 hPa, and the energy conversion terms (integrated in the vertical), are integrated over the regions of interest, i.e., tropical (10°N – 30°S, 30°W – 90°W) and the extratropical (30°S – 60°S, 30°W – 90°W) South America. To characterize the dominant temporal fluctuations in the energy terms, initially the annual cycle of the time series of each energy term was removed. The power spectrum of the time series of this energy terms was estimated by correlation coefficients, by fitting a "null" hypothesis continuum to the spectrum for Markov red noise persistence at 95% (Mitchell et al., 1966). The procedure for computing power spectrum for this method is given in

Lima (1996). The periodicities thus obtained were confirmed applying a 4th order Butterworth bandpass filter (Murakami, 1979), considering different frequency bands and the statistical significance at 90% and 95% was calculated through χ^2 distribution.

To analyze the energy conversions between the temporal scales, seasonal (91 days), intraseasonal (fluctuations with periods between 7 and 91 days) and high frequency (fluctuations associated with the transient disturbances, in this case with periods less than 7 days), we used Mak's local energetics scheme (Mak, 1991). The equation that governs the kinetic energy associated with the intraseasonal component of the flow, can be expressed as:

$$\left\langle \frac{\partial K_1}{\partial t} \right\rangle = \langle \mathbf{V}_1 \cdot \mathbf{A}_{0,1} \rangle + \langle \mathbf{V}_1 \cdot \mathbf{A}_{1,1} \rangle + \langle \mathbf{V}_1 \cdot \mathbf{A}_{1,2} \rangle + \langle \mathbf{V}_1 \cdot \mathbf{A}_{2,2} \rangle - \langle \mathbf{V}_1 \cdot \nabla\Phi_1 \rangle + \langle \mathbf{V}_1 \cdot \mathbf{F}_1 \rangle \quad (7)$$

The left-hand side of Eq. (7) represents the temporal variation of the kinetic energy of the intraseasonal component. The first four terms on the right-hand side of Eq. (7) denote the advective terms resulted from interactions between three temporal scales considered, and their sum is defined by symbol SAT. The term $\langle -\mathbf{V}_1 \cdot \nabla\Phi_1 \rangle$ denotes the contribution from episodal average of the work done by the pressure-gradient force, i.e., it expresses the role of the vertical circulations in the release of APE , associated with upward/downward motion of the relatively warm/cold air. The term $\langle \mathbf{V}_1 \cdot \mathbf{F}_1 \rangle$ is a measure of the local frictional dissipation rate. The subscripts 0, 1 and 2 represent the temporal scales, seasonal, intraseasonal and high-frequency components, respectively. The brackets denote the episodal averages (91 days) of each quantity. The interactions terms $\mathbf{A}_{0,1}$, $\mathbf{A}_{1,1}$, $\mathbf{A}_{1,2}$, $\mathbf{A}_{2,2}$ are defined in Mak (1991).

Here, all the terms in Eq.(7) were computed for summer seasons of the 1986–1987 and 1988–1989, except the term $\langle \mathbf{V}_1 \cdot \mathbf{F}_1 \rangle$, which was evaluated as a residue by assuming the left-hand side of Eq. (7) to be zero. The evaluation of budget of the local kinetic energy was made at 200 hPa level.

3 Results and discussion

3.1 Regional energetics

The mean values of \bar{K} , K_ψ and K_χ in (1) tropical and (2) extratropical regions of South America at levels 850 hPa and 200 hPa, for summer season are shown in Table 1. Analysis of this table shows that, in general, at both levels, the magnitude of K_ψ is slightly higher than \bar{K} , and at 200 hPa it is higher in area 2 than area 1. The energy terms \bar{K} , K_ψ and K_χ in the two regions show a maximum at 200 hPa where the strong westerlies (subtropical jet stream) exist. Thus, this result shows, as is well known, that K_ψ forms most of kinetic energy of the tropics and more so in the extratropics.

The temporal variations of \bar{K} , K_ψ and K_χ at 850 hPa are displayed in Fig. 1. This figure shows that the magnitude of K_χ at 850 hPa is low in all years, in both areas. \bar{K} and K_ψ

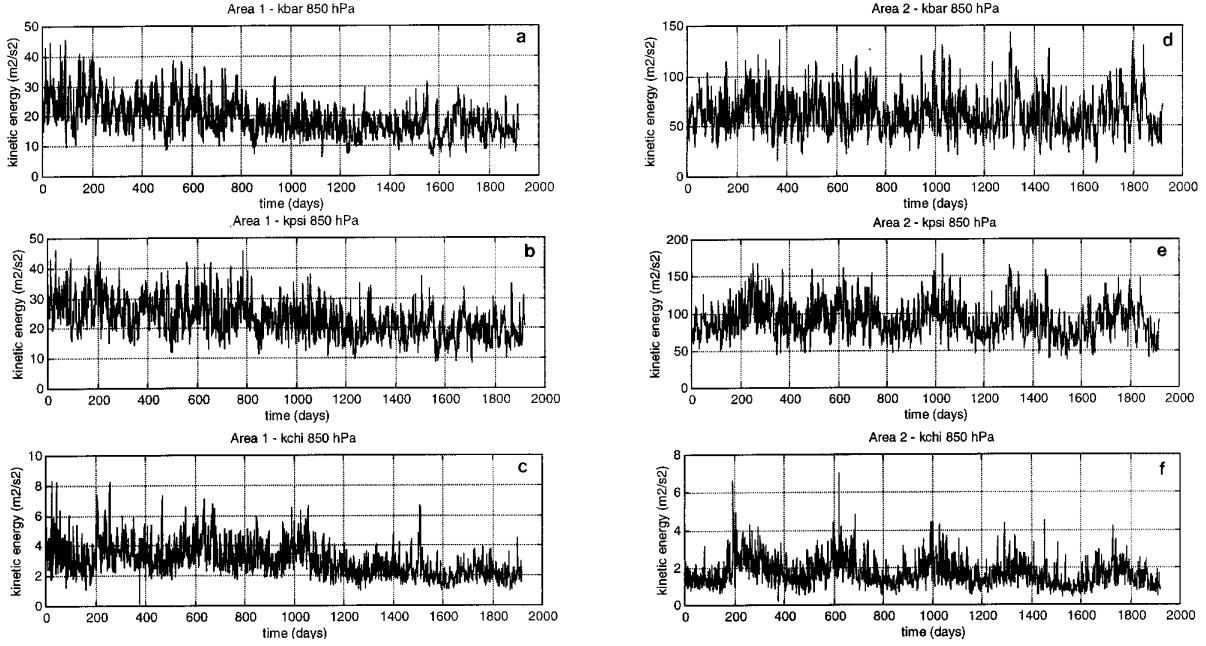


Fig. 1. Temporal variations of the kinetic energy (m^2s^{-2}) at 850 hPa, mean for tropical South America: (a) \bar{K} , (b) K_ψ , (c) K_χ , and extratropical South America: (d) \bar{K} , (e) K_ψ and (f) K_χ . Zero represents 1 November 1985.

Table 1. Mean values of the kinetic energies \bar{K} , K_ψ and K_χ , and the ratios K_χ/K_ψ , in areas (1) tropical and (2) extratropical South America, at levels 850 hPa and 200 hPa, for summer. Values are expressed in m^2s^{-2}

Regions	Levels (hPa)	Energy terms			
		\bar{K} m^2s^{-2}	K_ψ m^2s^{-2}	K_χ m^2s^{-2}	K_χ/K_ψ
1	850	20.64	24.42	3.04	0.12
1	200	109.14	150.8	9.95	0.065
2	850	58.47	81.12	1.35	0.017
2	200	390.47	468.38	3.3	0.007

show magnitudes larger than K_χ , being larger in area 2 than in area 1. At 200 hPa (Fig. 2) we note that the time variation of K_χ is low, but larger in area 1 than in area 2. The magnitude of K_χ is small compared to the magnitudes of \bar{K} and K_ψ at all the times, in both lower and upper levels. This means that there is no storage of K_χ , and K_χ is converted immediately to K_ψ , which indicates the catalytic role in the conversion of APE to the K_ψ . This was also noted by Chen and Wiin-Nielsen (1976).

Another aspect of the analysis of time series of the terms \bar{K} , K_ψ and K_χ at levels 850 hPa and 200 hPa (Figs. 1 and 2, respectively) is the dominant annual cycle in K_ψ and K_χ at 850 hPa, which is better defined in area 2 (extratropics) than in area 1 (tropics). Also, the annual cycle of the energy parameters is better defined at 200 hPa. We note that the max-

ima in annual cycle in K_ψ and K_χ occur in austral winter and the annual cycle of K_χ at 200 hPa is dominant and more distinct in area 1 than in area 2. In addition, we note inter-annual variations of \bar{K} , K_ψ and K_χ at 200 hPa in both the magnitude and the time of occurrence.

Area-time averaged kinetic energy components and conversions terms are given in Table 2, for summer seasons, in tropical and extratropical South America. This table shows that the dominant conversion term in the budget equations of K_ψ and K_χ over South America, in all summers, is the Coriolis term, denoted as $f\nabla\psi \cdot \nabla\chi$, with positive sign, indicating a conversion of K_χ into K_ψ . The other terms are of smaller magnitudes. The signs of the energy conversion terms $C(APE, K_\chi)$ and $C(K_\chi, K_\psi)$ are positive, indicating that the direction of the energy conversion is, as expected $APE \rightarrow K_\chi \rightarrow K_\psi$. Exception is noted in summer 3, when the term $C(APE, K_\chi)$ is negative but is of small magnitude, on order of $-0.9 \times 10^{-4} \text{ m}^2\text{s}^{-3}$, while the term $C(K_\chi, K_\psi)$ is positive and shows larger magnitude (values on order of $1.15 \times 10^{-4} \text{ m}^2\text{s}^{-3}$). In this summer, the direction of the energy exchange is $APE \leftarrow K_\chi \leftarrow K_\psi$.

A strong positive contribution of the zonal part of $C(APE, K_\chi)$ is noted during the summer in region 2. If the spectrum of the APE and K were separated in zonal and eddy components, it seen that most of APE is in zonal part (Sheng and Hayashi, 1990). The circulations of Hadley and Ferrel contribute for the conversion between APE and K of the zonal motion (Grotjham, 1993). Lambert (1989) calculated the global balance of K_ψ and K_χ considering the partition of this balance in zonal and eddy components. He noted that in individual years the conversion between zonal APE

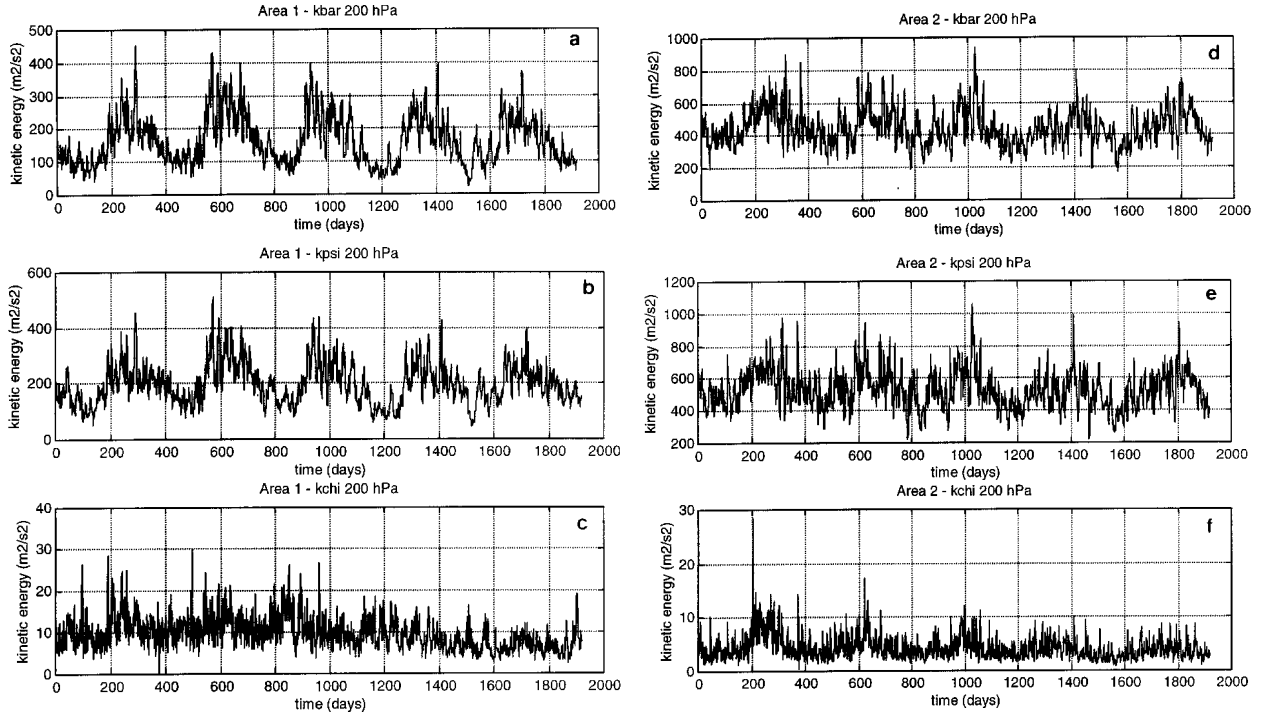


Fig. 2. Temporal variations of the kinetic energy (m^2s^{-2}) at 200 hPa, mean for tropical South America: (a) \bar{K} , (b) K_ψ , (c) K_χ , and extratropical South America: (d) \bar{K} , (e) K_ψ and (f) K_χ . Zero represents 1 November 1985.

Table 2. Area-time averaged kinetic energy terms for summers in (1) tropical and (2) extratropical domains of South America. Values are multiplied by $10^{-4} \text{m}^2\text{s}^{-3}$

Region 1	Energy conversions terms					
	Seasons	$\langle\langle f \nabla \psi \cdot \nabla \chi \rangle\rangle$	$\langle\langle \nabla^2 \psi \nabla \psi \cdot \nabla \chi \rangle\rangle$	$\frac{1}{2} \langle\langle \nabla^2 \chi (\nabla \psi)^2 \rangle\rangle$	$\langle\langle \omega J(\psi, \frac{\partial \chi}{\partial p}) \rangle\rangle$	$\langle\langle C(APE, K_\chi) \rangle\rangle$
1 (NDJF 85–86)	1.139	-0.14	-0.062	0.024	0.316	0.961
2 (NDJF 86–87)	1.332	-0.155	-0.017	0.033	0.480	1.193
3 (NDJF 87–88)	1.498	-0.293	-0.116	0.065	-0.087	1.154
4 (NDJF 88–89)	1.112	-0.225	-0.077	0.041	0.163	0.852
5 (NDJF 89–90)	1.507	-0.204	0.009	0.041	0.810	1.352
Mean	1.318	-0.203	-0.053	0.041	0.336	1.104
Region 2						
Seasons						
1 (NDJF 85–86)	2.130	-0.151	-0.260	0.012	2.623	1.732
2 (NDJF 86–87)	3.278	-0.083	-0.133	0.024	3.757	3.088
3 (NDJF 87–88)	2.769	0.011	-0.068	0.020	3.072	2.732
4 (NDJF 88–89)	3.214	0.129	0.019	0.004	3.273	3.368
5 (NDJF 89–90)	2.438	-0.0003	0.028	0.021	2.328	2.488
Mean	2.766	-0.0188	-0.083	0.016	3.011	2.680

and K_χ is dependent on season: in January the conversion is direct, furnishing energy to drive the divergent circulations (of the Hadley type and east-west) and, in July the conversion is opposite. He stresses the role of Ferrel circulation in this last conversion. Most of zonal part of K_χ at upper levels is due to Hadley circulation and the smaller contribution

of this term is due to Ferrel circulation. This strong positive contribution of the term $C(APE, K_\chi)$ indicates that the divergent circulation is important in this season. Also it can be noted in the tropics (area 1) the conversion from APE to K_χ is less than the conversion from K_χ to K_ψ . From Eq. 2 this implies a decrease with time of K_χ . The time tendency

term $\partial K_\chi/\partial t$ in general is close to zero. Thus, this implies an influx of divergent energy (B_χ) into the region. Table 2 also shows that in extratropics of South America the term $C(APE, K_\chi)$ is larger than the term $C(K_\chi, K_\psi)$, again this implies a boundary out flux of K_χ , in order to keep $\partial K_\chi/\partial t$ close to zero.

In the midlatitude regions a balance occurs between the horizontal advection of temperature and the adiabatic term, while in the tropics a balance occurs between the diabatic term and adiabatic term and the APE generated is immediately converted into K_χ . The immediate conversion between K_χ and K_ψ occurs because in the tropical troposphere the horizontal gradients of temperature are very weak and the local temporal variation of temperature is very small. With good approximation, the thermodynamic energy equation reduces to the balance between the adiabatic cooling term and the diabatic heating term (Holton, 1992). This result was confirmed by Nitta (1970) through a study of heat balance in Marshall Island area. He found that, for all frequency bands, the eddy EPD is generated by the heat of condensation, mainly by the release of the latent heat of condensation and is immediately converted to eddy kinetic energy.

Another aspect we note in Table 2 is that the kinetic energy budget over South America during the summer does not vanish. A similar result was also observed in earlier works, for example, Chen and Wiin-Nielsen (1976), Chen (1980), Lambert (1989), and others. Chen and Wiin-Nielsen (1976) noted that the discrepancy is larger in tropics than subtropics due to the stationary mode. Smith (1970) discussed the implications of calculating energy budgets in open systems. To justify the inconsistency observed in kinetic energy cycle over South America, two possibilities can be raised. One of them is the importance of the lateral boundary energy fluxes and the other, problems involved in the NMC analysis. Kanamitsu and Saha (1995) evaluated the systematic errors existent in NMC's analysis. Their results show a reduction of the K_ψ and EPD in all scales, mainly the small and medium scales. Approximately 50% of this reduction of energy is explained by excess of horizontal and vertical diffusion. The remaining part of this energy reduction can be related to the generation of EPD . This occurs probably due to the parametrization used for cumulus convection (Kuo scheme), which is a sink of EPD in small and medium scales. In spite of the mentioned inconsistency in the kinetic energy budget over South America, the results are still useful to understand the nature of the summer circulation over South America.

In order to put the results of Table 2 into a broader perspective, we have prepared the energy cycle diagram for tropics and extratropics of South America, given in Fig. 3. The larger boxes refer to the energy exchange components defined in Sect. 2 and the arrows show the overall direction of the conversion rates.

This regional energetics analysis shows that the main features of the atmosphere circulation over South America confirm earlier results. Also, the results presented in Table 2 show that the kinetic energy cycle over South America during the summer season is: $APE \rightarrow K_\chi \rightarrow K_\psi$.

According Lenters and Cook (1997), most of the structure of the atmosphere circulation in upper levels over South America during the summer is associated with the heat of condensation. Thus, a possible physical mechanism that explains the summer circulations over this region is that a heat source over South America would generate APE , through mainly latent heat of condensation which gets converted into K_χ through direct thermal circulation, represented by the term $-\chi \nabla^2 \Phi$, and this to K_ψ through the term $(f + \zeta) \nabla \psi \cdot \nabla \chi$.

3.2 Periodicities in the energetics

A visual examination of the energetic terms in Figs. 1 and 2 show the existence of some dominant periodicities. Thus, it would be interesting to make a systematic study of the periodicities in the energetics of summer circulation over South America. The periodicities obtained using FFT (Fast Fourier Transform) were confirmed through an estimated spectrum of statistically significant terms at 90% and 95%, using the method described by Mitchell et al. (1966). These results are very similar and some of them are presented to illustrate the method of Mitchell et al. (1966) and displayed in Fig. 4. Similar figures (not shown) are prepared for all the terms and for all five summers, both for areas 1 and 2.

The periodicities calculated by the method of Mitchell et al. (1966) were confirmed with the 4th order Butterworth filter, considering different frequency bands. The peaks obtained by the two methods are very similar. Table 3 shows these results for the summer season in the (1) tropical and (2) extratropical areas over South America. We included in this table only dominant (significant at 90% and 95%) periodicities between 20–60 days. This table shows large interannual variability. That is, only in some years were dominant periodicities observed in all the terms of the budget equations of K_χ and K_ψ , in the two study domains. Since the Madden-Julian Oscillation can occur both in the χ and ψ (Geisler and Pitcher, 1988; Chen and Chen 1997), one would expect the signal of MJO in the energy interactions terms also, although with periodicities different from those of χ and ψ .

From Table 3 it can be seen that the term K_ψ , which contains most of kinetic energy over tropical South America at 200 hPa in several years shows significant periodicities of around 20 days and 30–40 days. In extratropical South America, this term shows a peak of 20 days only in the summer of 1989–1990.

One good indicator of convective activity and the tropical heating is upper tropospheric divergence. The term K_χ at 200 hPa represents the kinetic energy associated with divergent part of the tropical circulation. This term shows dominant periodicity of around 30 days in area 1 in summer 4 (NDJF 1988–1989). In area 2, K_χ did not show any dominant periodicities in the range 20–60 days.

The term $-\chi \nabla^2 \Phi$ expresses the conversion between APE and K_χ (direct/indirect thermal circulation of warm/cold air rising and cold/warm air sinking, respectively). The analysis of the periodicities in this term shows peaks of around

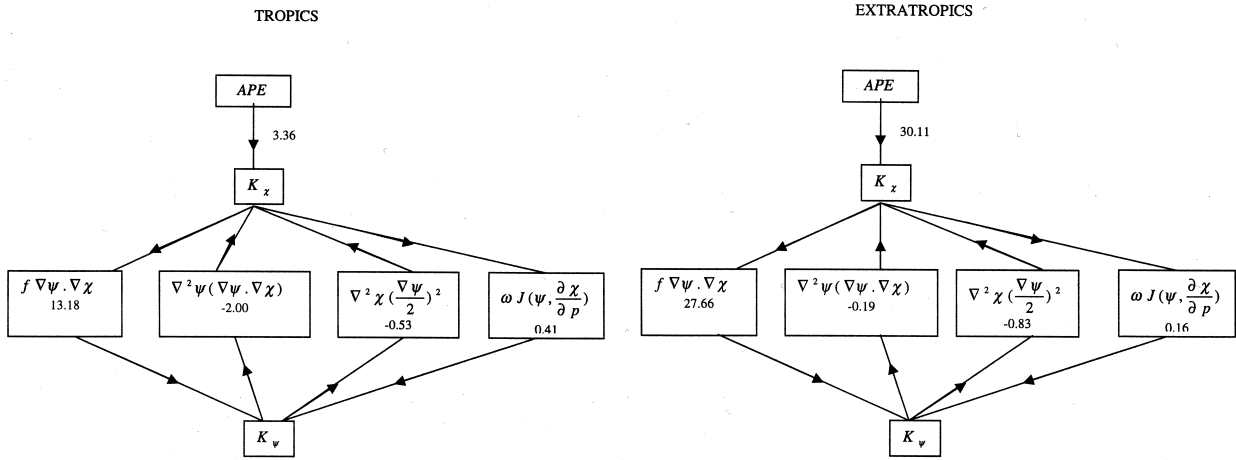


Fig. 3. Schematic energy cycle diagram of the atmospheric system. Arrows denote the most likely direction of the conversion between energy components for (a) tropical and (b) extratropical South America. Values of energy exchanges are within the boxes. The values are multiplied by $10^{-3} \text{ m}^2 \text{ s}^{-3}$.

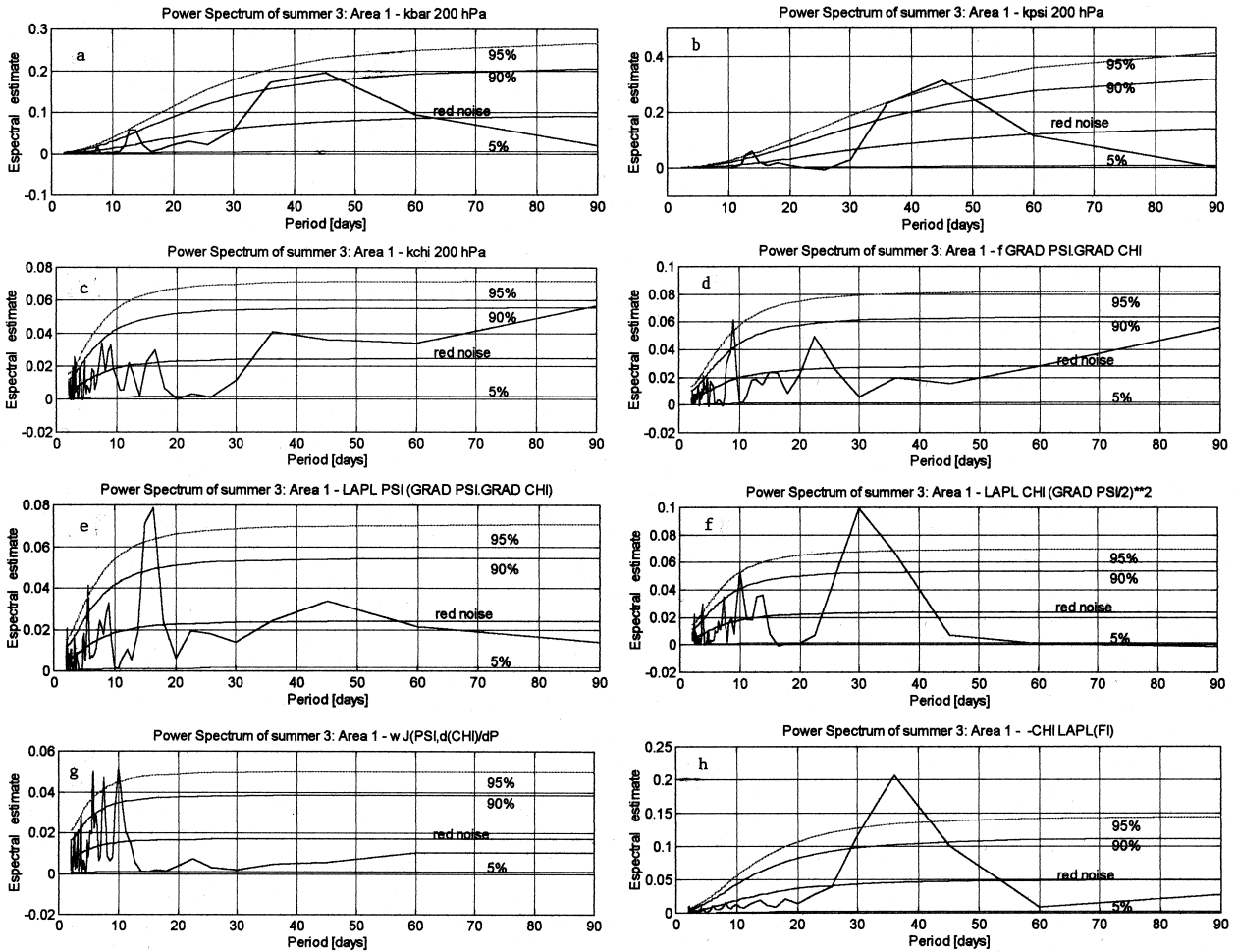


Fig. 4. Power spectrum estimated by method of Mitchell et al. (1966) in summer 3 in the area 1 for the terms: (a) \overline{K} at 200 hPa, (b) K_ψ at 200 hPa, (c) K_χ at 200 hPa, (d) $f\nabla\psi \cdot \nabla\chi$, (e) $\nabla^2\psi \nabla\psi \cdot \nabla\chi$, (f) $\frac{1}{2}\nabla^2\chi \nabla^2\psi$, (g) $\omega J(\psi, \frac{\partial\chi}{\partial t})$, (h) $-\chi \nabla^2\Phi$.

Table 3. Dominant periodicities in the energy parameters during five summers (NDJF 1985–1986, 1986–1987, 1987–1988, 1988–1989, 1989–1990) over tropical and extratropical South America. Values are expressed in days

Energy terms	Tropics					Extratropics				
	1	2	3	4	5	1	2	3	4	5
\bar{K} at 200 hPa	-	-	45*	-	-	-	-	-	-	20**
K_ψ at 200 hPa	35*	21*	43**	36*	-	-	-	-	-	20**
K_χ at 200 hPa	-	-	-	30*	-	-	-	-	-	-
$\langle\langle f\nabla\psi \cdot \nabla\chi \rangle\rangle$	-	25*	-	-	30*	-	-	-	22**	26**
$\langle\langle \nabla^2\psi \nabla\psi \cdot \nabla\chi \rangle\rangle$	25*	31**	-	44**	-	-	-	30**	-	22**
$\langle\langle \frac{1}{2}\nabla^2\chi \nabla^2\psi \rangle\rangle$	-	-	33*	29**	-	-	-	-	-	22*
$\langle\langle \omega J(\psi, \frac{\partial\chi}{\partial p}) \rangle\rangle$	23**	22* (37*)	-	36**	-	26**	-	35*	-	-
$\langle\langle -\chi \nabla^2\Phi \rangle\rangle$	29**	30*	28**	27*	-	-	-	36**	-	30**

The symbols (*), (**), and (-) denote significance at level 90%, 95% and not significant at 90% or 95%, respectively. The number 1, 2, 3, 4 and 5 denote the five summers, respectively.

30 days in all summers in the tropics, except in summer 5 (NDJF 1989–1990). In the extratropics of South America values of the periodicities ranging from 30 and 36 days were observed in individual years for the same term.

The term which explains most of the energy conversion between K_χ and K_ψ over South America is $f\nabla\psi \cdot \nabla\chi$. This term in tropical South America, in individual years, shows periodicities on the order of 20–30 days. In the extratropics of South America smaller periodicities were observed for the term $f\nabla\psi \cdot \nabla\chi$, varying in individual years from 22 days to 26 days.

Other dominant periodicities in energy conversion terms in area 1 are observed in the terms $\frac{1}{2}\nabla^2\chi(\nabla\psi)^2$ (with values of 29 and 33 days), $\omega J(\psi, \partial\chi/\partial p)$ (values in the range 22 and 37 days) and $\nabla^2\psi \nabla\psi \cdot \nabla\chi$ (values in the range 25 and 44 days), as can be seen in Table 3. Analyzing dominant oscillations in the energy parameters in area 2 we note periodicities of around 30 days in term $\nabla^2\psi \nabla\psi \cdot \nabla\chi$ and values of 26 and 35 days were observed in individual years in $\omega J(\psi, \partial\chi/\partial p)$.

Comparing results for the areas 1 and 2 (Table 3) we noted dominant oscillations with a 20–60 days period, both in tropical and extratropical latitudes of South America. This is similar to that noted by other authors for regions other than South America reviewed by Madden and Julian (1994). During the summer, the MJO signal was dominant in the energy parameters associated with χ field. This confirms earlier results of Boer (1995) and Lambert (1990).

Due to the episodic character of MJO (Boer, 1995), a wide band of periodicities is noted (Wang and Xie, 1997), and the signal of this oscillation is clearly seen in the results of energy budget of intraseasonal K_χ and K_ψ (Lambert, 1990). We are suggesting that the oscillations observed in kinetic energy terms integrated over South America, of about 20–45 days (Table 3), can be associated with MJO. However, to establish the energy cycle of MJO it is necessary to make global calcu-

lations. Based on kinetic energy cycle discussed earlier, the existence of the dominant periodicities in the kinetic energy terms, mainly in $f\nabla\psi \cdot \nabla\chi$, $\nabla^2\psi \nabla\psi \cdot \nabla\chi$ and $-\chi \nabla^2\Phi$, and noting the considerations made in earlier works about the relationship between (a) the diabatic heating, (b) the latent heat through cumulus convection and (c) the existence of MJO in tropics and extratropics latitudes, we suggest that the same kinetic energy cycle probably is valid for this oscillation, at least in a regional context over South America during the summer season. In a recent study Chen and Yanai (2000) used the Tropical Ocean-Global Atmosphere (TOGA) Coupled Ocean-Atmosphere Response Experiment (COARE) data to study the energetics of the MJO. They also found a similar energy cycle for the MJO.

The occurrence of MJO signal in the extratropics in summer is associated with the strong zonal wind (jet) in this region (Dasheng and Wenzhong, 1995). These authors suggest that the origin of MJO in these latitudes is due to a local instability. Thus a local energetic analysis on the lines suggested by Mak (1991) will be of interest in this context. Local energetics will be discussed in the next section.

3.3 Local kinetic energy balance

To clarify the dynamical nature of MJO over South America, we consider a local energetic analysis of Mak (1991) attempting to examine how the MJO interacts with the others dominant modes over South America (such as seasonal and high-frequency variations). This analysis is made over the whole of South America because the MJO signal arises both in tropical and extratropical latitudes. Further, through the local energetic analysis one can identify how much energy is due to the energy conversion and how much is due to the energy propagation.

For the local energetic analysis we consider two summers: DJF 1986–1987 and 1988–1989. These summers are consid-

ered here because these were seasons when the atmospheric circulation was anomalous on a global scale, characterized by drought and flood conditions over South America, respectively (Rao et al., 1998). The year 1987 was characterized by moderate El Niño phenomenon and the summer of 1988–1989 was characterized by the La Niña phenomenon (Climanálise, 1986, 1987, 1988, 1989).

3.3.1 Local kinetic energy considerations

Kinetic energy field of the three components (K_0 , K_1 and K_2 , respectively) in both summers (Fig. 5) shows that the maximum K_0 is located in extratropical latitudes and approximately corresponds to the location of the subtropical jet stream over South Atlantic and southeast Pacific Ocean (Figs. 5a and 5d, respectively). This result confirms what was noted by Eastin and Vincent (1998). In the summer of 1986–1987 (Fig. 5b) there is a center of episodic energy (K_1) with values on order of $105 \text{ m}^2\text{s}^{-2}$. This center is located approximately at 55°W between 30°S and 60°S , and coincides with the region of SACZ, with a northwest-southeast orientation. Other centers of maximum values are noted in the southeast Pacific Ocean (80°W , between 30°S and 40°S) and South Atlantic Ocean (in 30°W , between 50°S and 60°S), with magnitudes about $90 \text{ m}^2\text{s}^{-2}$ and $75 \text{ m}^2\text{s}^{-2}$, respectively. In the summer of 1988–1989 the center of the maximum K_1 located in the southeast of South America is much weaker (values on order of $45 \text{ m}^2\text{s}^{-2}$), and more zonally oriented over the same region. The K_2 spatial field shows that the high frequency is more dominant in midlatitudes in both the summers (Figs. 5c and 5f, respectively), and shows several centers of K_2 in this region.

Figure 6 shows the spatial distribution of the advective terms in the local budget equation for K_1 . The comparison of magnitude of these terms for both summers indicate that the $\langle \mathbf{V}_1 \cdot \mathbf{A}_{0,1} \rangle$ is the dominant term, which represents the interactions among the seasonal and intraseasonal components. This result was expected since the two components have most of the variance. Also, we note a local wave train from the Pacific to South Atlantic Ocean, oriented southwest-northeast, better defined and stronger in terms $\langle \mathbf{V}_1 \cdot \mathbf{A}_{0,1} \rangle$ and $\langle \mathbf{V}_1 \cdot \mathbf{A}_{1,1} \rangle$ in the summer of 1986–1987 than in the summer of 1988–1989. This southwest-northeast pattern is very similar to the pattern noted by Nogués-Paegle and Mo (1997) (their Fig. 9) in 200 height differences associated with see-saw patterns in rainfall over South America. Nogués-Paegle and Mo (1997) suggested the possible link of this see-saw pattern to 30–60 days intraseasonal oscillation. Our results of investigation into energetics suggest that this see-saw pattern is probably generated by the interaction of seasonal and intraseasonal components over South America. Further, in the summer of 1988–1989, we observed a maximum positive center in the term $\langle \mathbf{V}_1 \cdot \mathbf{A}_{0,1} \rangle$, with values on the order of $2.5 \times 10^{-3} \text{ m}^2\text{s}^{-3}$, located on west coast of South America (90°W , 5°S). This also is noted in the term $\langle \mathbf{V}_1 \cdot \mathbf{A}_{1,1} \rangle$, but it is weaker. Figures 6d and 6h show that the high frequency is dominant in midlatitudes in both the summers, as noted by

the term $\langle \mathbf{V}_1 \cdot \mathbf{A}_{2,2} \rangle$.

Following Mak (1991) the term $\langle \mathbf{V}_1 \cdot \mathbf{A}_{0,1} \rangle$ can be written as the sum of two terms: (1) a redistribution of the kinetic energy of the intraseasonal component due to the advection by the seasonal flow component $-(\mathbf{V}_0 \cdot \nabla) \langle K_1 \rangle$, and (2) a generation of kinetic energy by a barotropic process represented by the scalar product $\mathbf{E}_1 \cdot \mathbf{D}_0$. The \mathbf{E}_1 vector is a measure of the local structure of a disturbance (Lau, 1988) such that it gives the local shape and orientation of the intraseasonal component of the flow. The \mathbf{D}_0 vector is a measure of the deformation field of the seasonal flow component. The positive sign of $\mathbf{E}_1 \cdot \mathbf{D}_0$ means that the disturbance extracts kinetic energy from the basic flow. The negative sign implies the opposite. A breakdown of these processes can illustrate the role of interactions of scales in the redistribution of local energy. Thus, we may write, following Mak (1991):

$$\langle \mathbf{V}_1 \cdot \mathbf{A}_{0,1} \rangle = -(\mathbf{V}_0 \cdot \nabla) \langle K_1 \rangle + \langle \mathbf{E}_1 \cdot \mathbf{D}_0 \rangle \quad (8)$$

where

$$\mathbf{A}_{0,1} = -L_1 \{ (\mathbf{V}_0 \cdot \nabla) \mathbf{V}_1 + (\mathbf{V}_1 \cdot \nabla) \mathbf{V}_0 \} \quad (9)$$

$$\langle \mathbf{E}_1 \rangle = \frac{1}{2} \left(\langle v_1^2 \rangle - \langle u_1^2 \rangle - \langle u_1 v_1 \rangle \right) \quad (10)$$

$$\mathbf{D}_0 = (\mathbf{D}_{\text{st}}, \mathbf{D}_{\text{sh}}) \quad (11)$$

$$D_{\text{st}} = \frac{1}{a \cos \Phi} \frac{\partial u_0}{\partial \lambda} - \frac{1}{a} \frac{\partial v_0}{\partial \Phi} - \frac{v_0}{a} \tan \Phi \quad (12)$$

$$D_{\text{sh}} = \frac{1}{a \cos \Phi} \frac{\partial v_0}{\partial \lambda} + \frac{1}{a} \frac{\partial u_0}{\partial \Phi} + \frac{u_0}{a} \tan \Phi \quad (13)$$

where L_1 is linear operator in time that includes fluctuations with scales longer than a week but shorter than a season. \mathbf{V}_0 and \mathbf{V}_1 are horizontal velocity associated with seasonal and intraseasonal components, respectively. u_0 , v_0 are the seasonal zonal and meridional components of wind. λ is longitude, Φ is latitude, and a is the Earth's radius. The D_{st} and D_{sh} are the deformation fields components due the stretching and shearing of this field.

Figure 7 shows the spatial fields of the \mathbf{D}_0 and \mathbf{E}_1 vectors, the direction of these vectors, the spatial distribution of terms $\mathbf{E}_1 \cdot \mathbf{D}_0$ and $-(\mathbf{V}_0 \cdot \nabla) \langle K_1 \rangle$, into the two summers, respectively. As suggested from the field of direction of the \mathbf{D}_0 vector, in general, we note that locally the disturbance is oriented in the NW–SE direction, in both summers (Figs. 7a and 7g, respectively). This configuration indicates that \mathbf{D}_0 has a northward component of propagation. The direction of propagation of the intraseasonal component is related to the direction of the \mathbf{E}_1 vector. In summer of 1986–1987, the major axis of \mathbf{E}_1 is in NW–SE direction and in the summer of 1988–1989, this axis is in east-west direction (Figs. 7b and 7h, respectively). Both configurations indicate that these components in both the summers are propagating westward. Also, the shape of intraseasonal component in the summer of 1986–1987 indicates a wave-like disturbance.

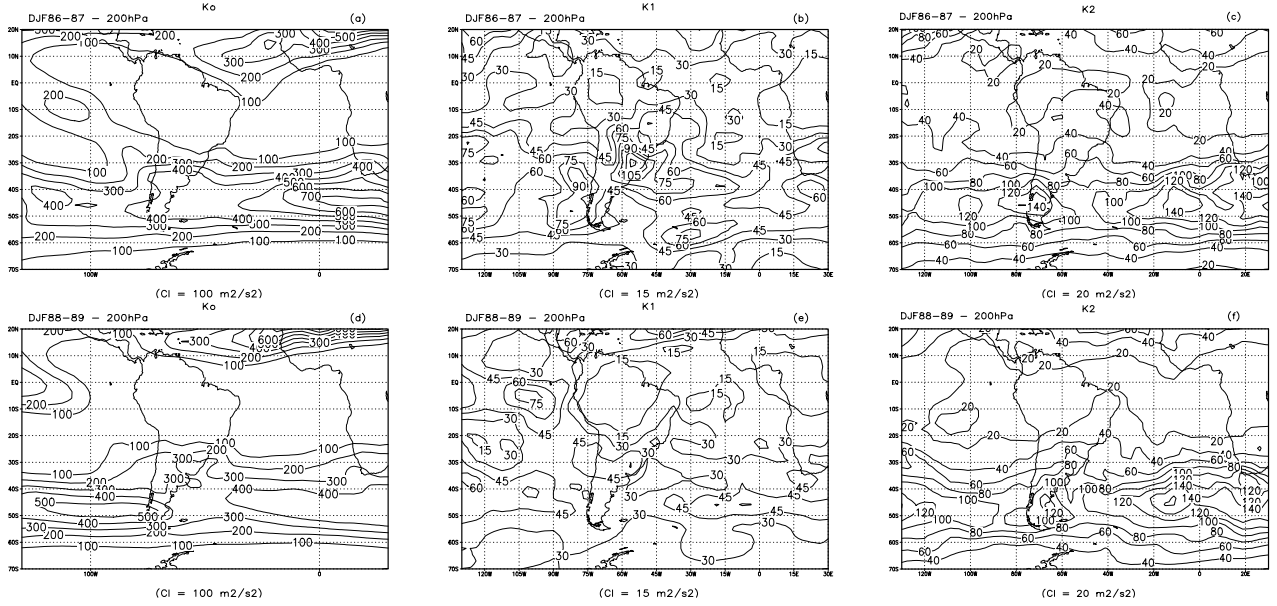


Fig. 5. Distribution of the episodal average kinetic energy at 200 hPa of the seasonal (left panels), intraseasonal (middle panels) and high frequency (right panels) components, in summers of 1986–1987 and 1988–1989, respectively. The values are expressed in m^2s^{-2} . CI stands for contour interval.

The orientation of \mathbf{D}_0 and \mathbf{E}_1 in the summers of 1986–1987 and 1988–1989 is such that it indicates the intraseasonal component would lose energy to the basic flow (Mak and Cai, 1989). Further, the intraseasonal component is acting to accelerate the flow where the arrows are divergent and retard the flow where the arrows are convergent. Figure 7d shows that in summer of 1986–1987, \mathbf{E}_1 is divergent in jet stream region, along about 40°S and 50°S and southeast Pacific and Atlantic Ocean. Also, in this summer, \mathbf{E}_1 is divergent in the region between the equator and 10°S , along 110°W , which coincides with the location of the other branch of subtropical jet stream. Between 40°S and 50°S , along 110°W , there is a larger convergence region which indicates that the mean flow is decreasing in this region. The divergent region in midlatitudes is more intense in the summer of 1986–1987 than in the summer of 1988–1989 (Figs. 7d and 7j, respectively).

We note that over most of South Atlantic Ocean and over continental part of South America the term $\mathbf{E}_1 \cdot \mathbf{D}_0$ shows strong negative values (values larger than $0.2 \times 10^{-3} \text{ m}^2\text{s}^{-3}$) during the summer of 1986–1987 (Fig. 8e). Some positive centers are noted in the Pacific Ocean, with magnitudes higher than $0.2 \times 10^{-3} \text{ m}^2\text{s}^{-3}$. In the summer of 1988–1989 a stronger positive center of $\mathbf{E}_1 \cdot \mathbf{D}_0$ is located off the west coast of South America, with a maximum value of $1.0 \times 10^{-3} \text{ m}^2\text{s}^{-3}$ (Fig. 7k), which is coincident with the low sea surface temperature region noted in La Niña of 1988–1989 event. Comparing the results shown in Figs. 6e, 7k and 7l, we note that the most part of the maximum center located in Pacific Ocean of term $\langle \mathbf{V}_1 \cdot \mathbf{A}_{0,1} \rangle$ in the summer of 1988–1989 is generated by $\mathbf{E}_1 \cdot \mathbf{D}_0$ term. In this summer, negative centers are observed both in the Pacific Ocean

(between 30°S and 50°S) and Atlantic Ocean, on the southwest coast of Africa and southwest coast of Brazil. The term $\langle -\mathbf{V}_0 \cdot \nabla \rangle \langle K_1 \rangle$ for the summer of 1986–1987 shows a local stronger wave train than in the summer of 1988–1989, with southwest-northeast orientation, eastward propagating from the Pacific to Atlantic Ocean (Figs. 7f and 7l, respectively). This pattern is similar to that noted in term $\langle \mathbf{V}_1 \cdot \mathbf{A}_{0,1} \rangle$ (Fig. 6a).

Figure 8 shows the spatial distribution of sum of the advective terms between three temporal scales (denoted by SAT), $\langle -\mathbf{V}_1 \cdot \nabla \Phi_1 \rangle$ and $\langle \mathbf{V}_1 \cdot \mathbf{F}_1 \rangle$. The SAT terms represent the net energy generation rate associated with the conversions between the three temporal components of the flow. This figure shows that the geographical location of the local maximum of SAT associated with these interactions occurs near the climatological position of the SACZ, oriented along northwest-southeast direction. Comparing the magnitude of SAT, $\langle -\mathbf{V}_1 \cdot \nabla \Phi_1 \rangle$ and $\langle \mathbf{V}_1 \cdot \mathbf{F}_1 \rangle$ for both summers, we note that the three terms have equal magnitudes. The term $\langle -\mathbf{V}_1 \cdot \nabla \Phi_1 \rangle$ is spatially opposite to that of SAT. Further, we note a wave pattern propagating with southwest-northeast direction, localized over the southern part of South America. Mak and Cai (1989) studied the problem of the jet stream instability without considering the separation into temporal scales. They note that locally, the advection (SAT) and energy generation $\langle -\mathbf{V}_1 \cdot \nabla \Phi_1 \rangle$ terms are in phase, such that the advection terms denote the process that redistributes the energy downstream of the maximum energy generation location. Further, the balance between of local kinetic energy and the processes of the energy redistribution determines the instantaneous location of the maximum wave activity. Thus, the opposite sign between $\langle -\mathbf{V}_1 \cdot \nabla \Phi_1 \rangle$ and

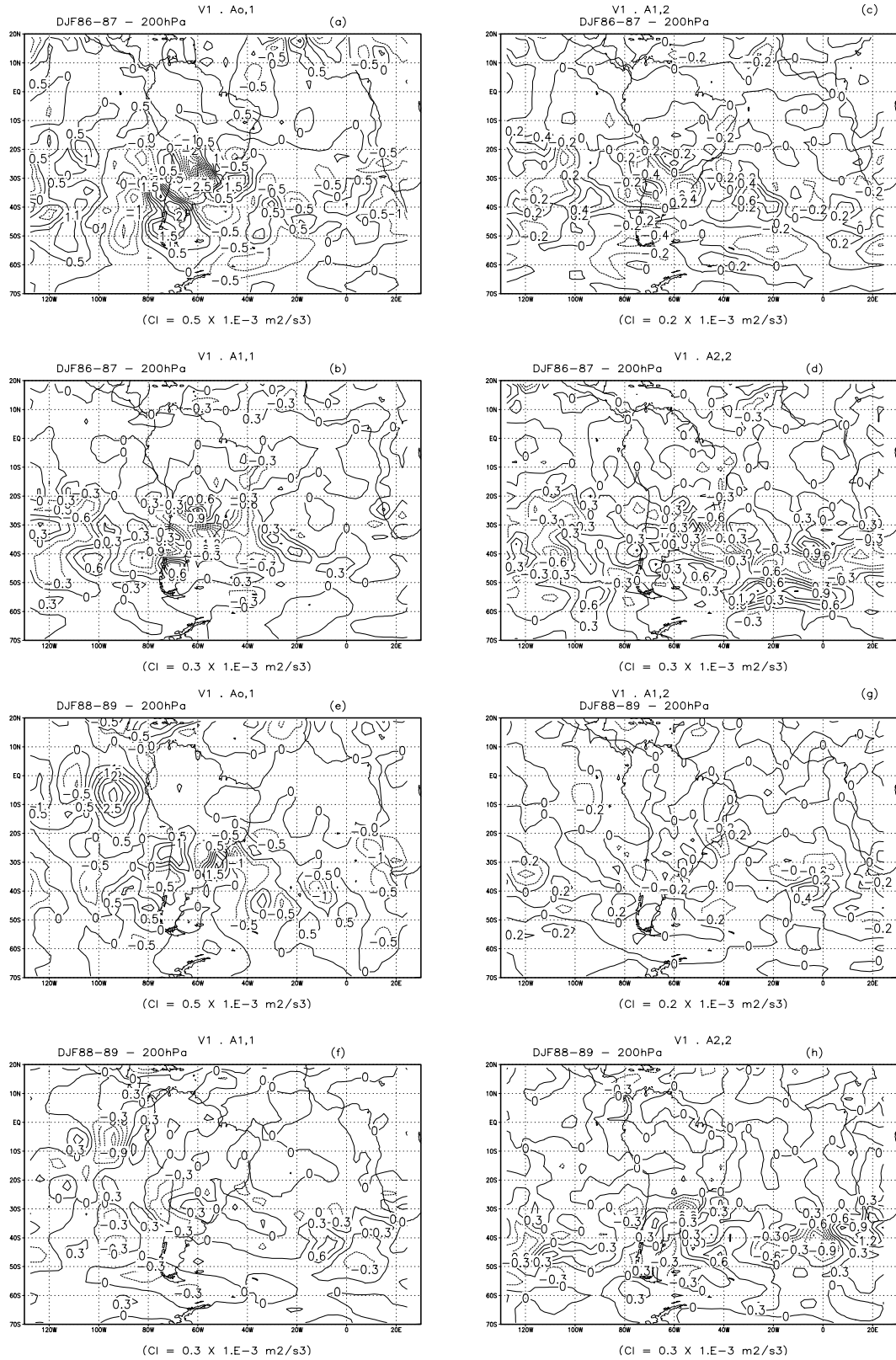


Fig. 6. Episodal average of the spatial distribution of the four individual advective terms in the summer of 1986–1987: (a) $\langle V_1 \cdot A_{0,1} \rangle$, (b) $\langle V_1 \cdot A_{1,1} \rangle$, (c) $\langle V_1 \cdot A_{1,2} \rangle$, (d) $\langle V_1 \cdot A_{2,2} \rangle$, and in the summer of 1988–1989: (e) $\langle V_1 \cdot A_{0,1} \rangle$, (f) $\langle V_1 \cdot A_{1,1} \rangle$, (g) $\langle V_1 \cdot A_{1,2} \rangle$, (h) $\langle V_1 \cdot A_{2,2} \rangle$. Values are multiplied by $10^{-3} \text{ m}^2 \text{ s}^{-3}$. CI stands for contour interval.

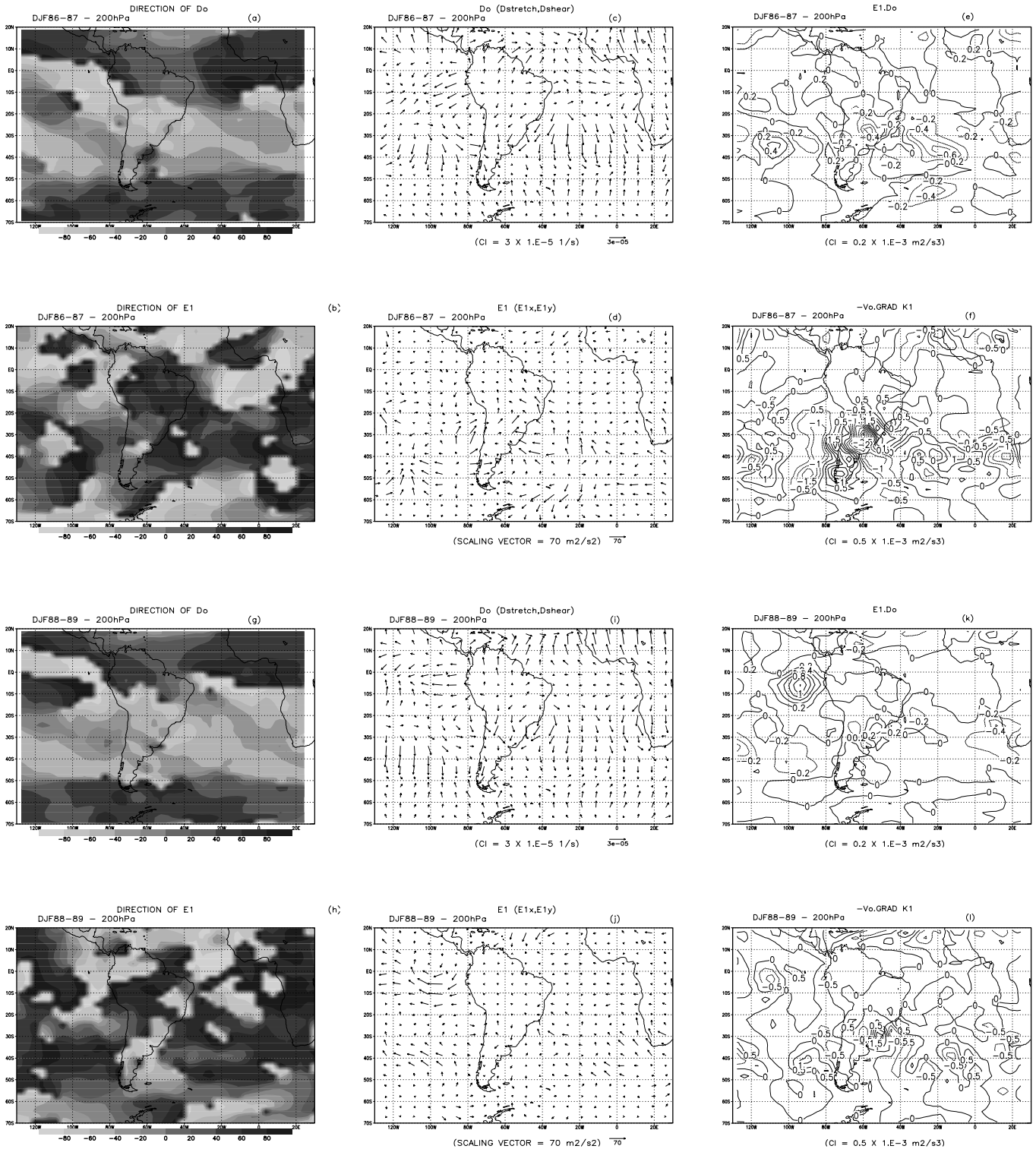


Fig. 7. In the upper six panels the episodal average of summer of 1986–1987 is shown for direction of the vectors: **(a)** D_0 , **(b)** E_1 , **(c)** $D(D_{st}, D_{sh})$, **(d)** $E_1(E_{1,x}, E_{1,y})$, and **(e)** the spatial distribution of the local barotropic energy generation rate ($E_1 \cdot D_0$) as well as **(f)** the spatial field ($-V_0 \cdot \nabla \langle K_1 \rangle$). Analogous to **(a) – (f)** the situation for the summer of 1988–1989 is presented in lower panels **(g) – (m)**.

SAT term means that the maximum episodic K_1 is generated by baroclinic processes essentially by term $(-V_1 \cdot \nabla \Phi_1)$, while SAT redistributes energy K_1 . A similar but weaker pattern is observed in the summer of 1988–1989.

As mentioned earlier, the main systems of the atmospheric circulation at 200 hPa over South America during the summer are BH and NL. Table 4 shows the integration of the local kinetic energy term in these two regions. Distinct dom-

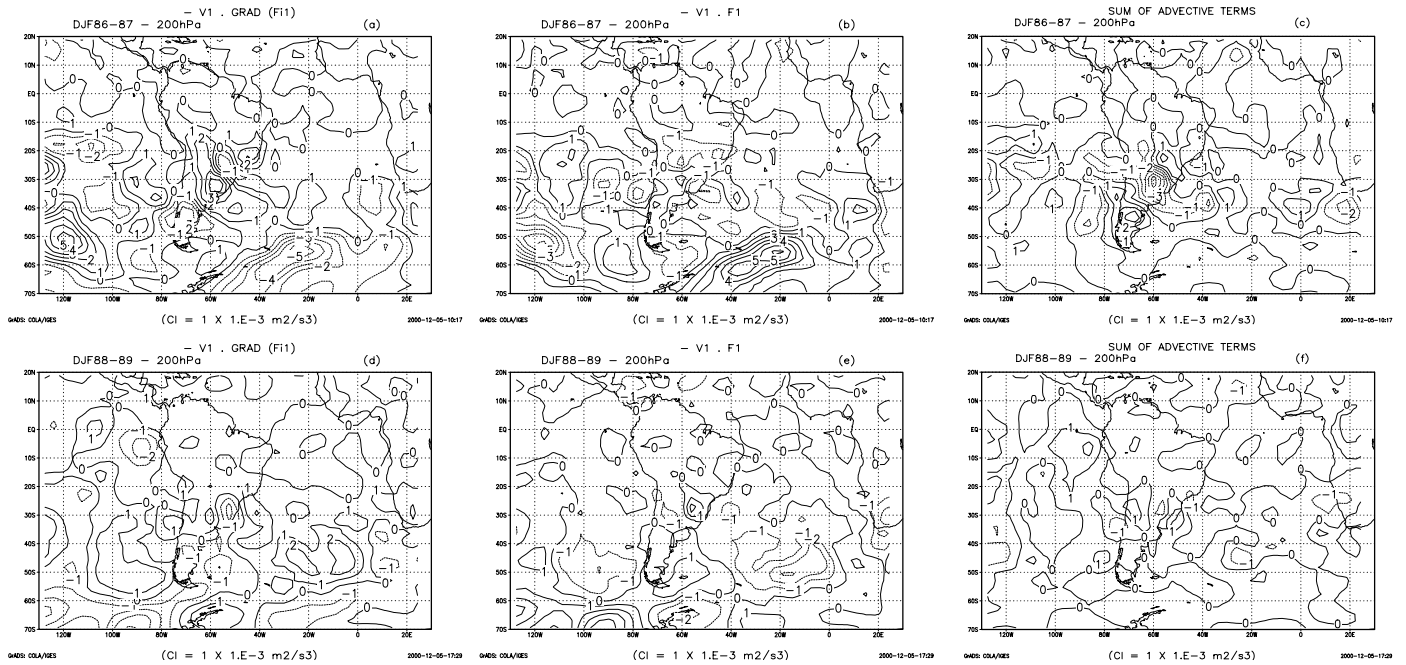


Fig. 8. Episodal average of the spatial distribution of (a), (d) $\langle -V_1 \cdot \nabla \Phi_1 \rangle$, (b), (e) $\langle V_1 \cdot F_1 \rangle$ and (c), (f) the sum of the four advective terms on the right-hand side of the kinetic energy equation (7) denoted as SAT, to summers of NDJF of 1986–1987 and 1988–1989, respectively.

inant interaction occurs between these systems in both the summers. In the summer of 1986–1987 in BH and NL, the stronger signal is observed in the term $\langle V_1 \cdot A_{0,1} \rangle$. Also, the term $\langle V_1 \cdot A_{1,2} \rangle$, which expresses interactions between intraseasonal and high frequency components, is stronger. These results show that in the BH region the dominant atmospheric circulation is the large scale one. In NL region, the upper circulation and the transient disturbances (for example, cyclone vortices of upper levels (Gan, 1983)) are important. However, we note that the dominant temporal scales are not the same in both summers.

As point out earlier, 1986–1987 and 1988–1989 years are El Niño and La Niña years, respectively. Rasmusson (1991) discussed the differences in the global atmospheric circulation in both summers. He noted that the divergent pattern over South American sector suggests relatively wet conditions over the eastern equatorial Pacific and dry conditions over northeastern South America during 1986–1987, and the reverse during 1988–1989. This result was also verified by Lima (1996), with the regional energetic analysis over South America. Further, Pezzi et al. (1996) noted that the jet stream of the South Hemisphere shows the seasonal and interannual variations in its climatological position. In general, during El Niño years, the jet stream is stronger than in La Niña years. This feature of the jet stream is observed in earlier works, such as Kousky et al. (1984) and Ambrizzi (1994), among others. Thus, our results show that, during the El Niño of 1986–1987, the increase in mean flow was largely due to contribution of intraseasonal component (as seen in Fig. 7) and the high divergence over South America (Lima, 1996)

helped to enhance and maintain the subtropical jet stream, by the Coriolis force, represented by term $f \nabla \psi \cdot \nabla \chi$. During the summer of 1988–1989, the divergence over the continent is stronger than summer of 1986–1987 (Lima, 1996), but the contribution of intraseasonal component to mean flow is weaker, acting to decelerate the jet stream in this summer.

4 Concluding remarks

We have analyzed the energetics of the atmospheric circulation over South America during the summer season. The study focuses on regional and local features. In addition, spectral analysis has been made to evaluate the dominant periodicities in energy terms. However, the main objective was to learn about the energy exchange processes and to understand how the atmospheric circulation over South America is maintained. The following conclusions emerge as reasonable interpretations of these results.

The regional energetic analysis showed the kinetic energy cycle in K_ψ and K_χ components and explained how the summer circulation over South America is maintained. The probable physical mechanism which explains this circulation could be: a heat source over South America to generate EPD , through latent heat of condensation which converts to K_χ through direct thermal circulation, represented by the term $-\chi \nabla^2 \Phi$, and this then to K_χ through the term $(f + \zeta) \nabla \psi \cdot \nabla \chi$. Another important aspect of this analysis was that several dominant periodicities were detected in energetic parameters, such as: (1) the annual cycle, better defined in upper levels, in both tropical and extratropical of

Table 4. Average contributions of the local energy balance equation terms, in summers of 1986–1987 and 1988–1989. Values are expressed in $1.0 \times 10^{-3} \text{ m}^2 \text{ s}^{-3}$

Bolivian High (10°S–20°S; 80°W–55°W) $\times 10^{-4} \text{ m}^2 \text{ s}^{-3}$							
Periods	$V_1 \cdot A_{0,1}$	$V_1 \cdot A_{1,1}$	$V_1 \cdot A_{1,2}$	$V_1 \cdot A_{2,2}$	SAT	$-V_1 \cdot \nabla \Phi_1$	$V_1 \cdot F_1$
NDJF 86–87	-1.78	0.65	-0.06	-0.04	-1.23	5.00	-3.77
NDJF 88–89	-1.73	-0.45	0.25	0.14	-1.79	4.46	-2.67

Northeast Brazil Low (10°S–20°S; 40°W–20°W) $\times 10^{-4} \text{ m}^2 \text{ s}^{-3}$							
Periods	$V_1 \cdot A_{0,1}$	$V_1 \cdot A_{1,1}$	$V_1 \cdot A_{1,2}$	$V_1 \cdot A_{2,2}$	SAT	$-V_1 \cdot \nabla \Phi_1$	$V_1 \cdot F_1$
NDJF 86–87	1.16	-0.51	-0.24	-0.22	0.19	1.07	-1.26
NDJF 88–89	-0.51	1.48	1.02	-0.18	1.81	-1.50	-0.31

South America, verified in all energy terms; (2) intraseasonal (30–60 day) oscillation and (3) oscillations of less than 20 days.

The most interesting features to emerge from the periodicities analysis were the occurrence of dominant peaks around 30 days observed in all energy terms, mainly the terms $f \nabla \psi \cdot \nabla \chi$, $\nabla^2 \psi \nabla \psi \cdot \nabla \chi$ and $-\chi \nabla^2 \Phi$. Spectral analysis of energy conversions terms permitted us to infer the kinetic energy cycle of MJO. Probably this cannot be achieved by spectral analysis of parameters such as ψ and χ .

In general, the results of local energy analysis showed that the dominant interactions between the three temporal scales over South America occur near or over SACZ region, showing NW–SE orientation, similar to the orientation of SACZ. Different scales are important over South America: over the Bolivian High, the main components are seasonal and intraseasonal, and over the Northeast Brazil Low, the intraseasonal and high frequency are important. This analysis also showed the relative importance of the baroclinic and barotropic processes in the dynamics of the summer circulation over South America.

Acknowledgements. This forms part of the PhD thesis of the first author. We acknowledge the computational support provided by CPTEC/INPE/MCT and the financial support from CNPq and FAPESP to the first author. Thanks are due to Prof. E. C. Kung and another anonymous reviewer for helpful comments. Thanks are also due to Dr. Carlos Nobre for his interest in this study.

Topical Editor Donal P. Murtagh thanks M. Kanamitsu and E. C. Kung for their help in evaluating this paper.

References

Ambrizzi, T., Rossby wave propagation on El Niño and La Niña non-zonal basic flows, *Rev. Brasil. Meteor.*, 8/9, 54–65, 1993/1994.

Boer, G. J., Analysed and forecast large-scale tropical divergent flow, *Mon. Weather Rev.*, 123, 3539–3553, 1995.

Chen, T.-C., On the energy exchange between the divergent and rotational components of atmospheric flow over the tropics

and subtropics at 200 mb during two northern summers, *Mon. Weather Rev.*, 108, 896–912, 1980.

Chen, T.-C. and Chen, J.-M., On the relationship between the streamfunction and velocity potential of the Madden-Julian Oscillation, *J. Atmos. Sci.*, 54, 679–685, 1997.

Chen, T.-C. and Wiin-Nielsen, A. C., On the kinetic energy of the divergent and nondivergent flow in the atmosphere, *Tellus*, 28, 486–498, 1976.

Chen, T.-C., Weng, S.-P., and Schubert, S., Maintenance of austral summertime upper-tropospheric circulation over tropical South America: the Bolivian High-Nordeste Low system, *J. Atmos. Sci.*, 56, 2081–2100, 1999.

Chen, B. and Yanai, M., Comparison of the Madden-Julian Oscillation (MJO) during the TOGA COARE IOP with a 15-year climatology, *J. Geophys. Res.*, 105, 2139–2149, 2000.

Climanálise São José dos Campos, INPE, 1–2, 1986–1987.

Climanálise São José dos Campos, INPE, 3–4, 1988–1989.

Dasheng, Y. and Wenzhong, C., A possible dynamics mechanism of the atmospheric 30–60 day oscillation in the extratropical latitude, *Chinese J. Atmos. Sci.*, 19, 102–112, 1995.

DeMaria, M., Linear response of a stratified tropical atmosphere to convective forcing, *J. Atmos. Sci.*, 42, 1944–1959, 1985.

Eastin, M. D. and Vincent, D. G., A 6-yr climatology of vertical mean and shear components of kinetic energy for the Australian-South Pacific jet stream, *J. Clim.*, 11, 283–291, 1998.

Figueroa, S. N. and Nobre, C. A., Precipitation distribution over central and western tropical South America, *Climanálise*, 5, 36–45, 1990.

Figueroa, S. N., Satyamurty, P., and Silva Dias, P. L., Simulation of the summer circulation over the South America region with an ETA coordinate model, *J. Atmos. Sci.*, 52, 1573–1584, 1995.

Gan, M. A., Um estudo observacional sobre as baixas frias da alta troposfera, nas latitudes subtropicais do Atlântico Sul e leste do Brasil. Dissertação de mestrado em meteorologia - INPE, São José dos Campos, INPE–2685–TDL/126, 1983.

Gandu, A. W. and Geisler, J. E., A primitive equation model study of the effect of topography on the summer circulation over tropical South America, *J. Atmos. Sci.*, 52, 1573–1583, 1991.

Geisler, J. E. and Pitcher, E. J., On the representation of the 40–50 day oscillation in terms of velocity potential and streamfunction, *J. Atmos. Sci.*, 45, 1850–1854, 1988.

Grotjahn, R., *Global atmospheric circulations – observations and theories*, New York, Oxford University Press, 1993.

- Gutman, G. and Schwerdtfeger, W., The role of latent and sensible heat for the development of high pressure system over the subtropical Andes, in the summer, *Meteorol. Rundschau*, 18, 69–75, 1965.
- Holton, J. R., An introduction to dynamic meteorology, 3rd ed., San Diego, Academic Press, 1992.
- Kanamitsu, M. and Saha, S., Spectral budget analysis of the short-range forecast error of the NMC medium-range forecast model, *Mon. Weather Rev.*, 123, 1834–1850, 1995.
- Kleeman, R., A modeling study of the effect of the Andes on the summertime circulation of tropical South America, *J. Atmos. Sci.*, 46, 3344–3362, 1989.
- Kousky, V. E., Kagano, M. T., and Cavalcanti, I. F. A., A review of the Southern Oscillation: oceanic-atmospheric circulation changes and related rainfall anomalies, *Tellus*, 36A, 490–504, 1984.
- Krishnamurti, T. N. and Ramanathan, Y., Sensitivity of the monsoon onset to differential heating, *J. Atmos. Sci.*, 39, 1290–1306, 1982.
- Krishnamurti, T. N., Sinha, M. C., Jha, B., and Mohanty, U. C. A study of South Asian monsoon energetics, *J. Atmos. Sci.*, 55, 2530–2548, 1998.
- Lambert, S. J., A divergent and rotational kinetic energy budget for January and July, *J. Geophys. Res.*, 94, 11 137–11 149, 1989.
- Lambert, S. J., Observed and simulated intraseasonal energetics, *J. Clim.*, 3, 1330–1346, 1990.
- Lau, N. C., Variability of the observed midlatitude storm tracks in relation to low frequency changes in the circulation pattern, *J. Atmos. Sci.*, 45, 2718–2743, 1988.
- Lenters, J. and Cook, K. H., On the origin of the Bolivian High and related circulation features of the South America climate, *J. Atmos. Sci.*, 54, 656–677, 1997.
- Lima, M. C. Manutenção da circulação atmosférica sobre a América do Sul. PhD Thesis in Meteorology, São José dos Campos, INPE, (INPE-6646- TDI/623), 1996.
- Madden, R. A. and Julian, P. R., Observations of the 40–50 day tropical oscillation – a review, *Mon. Weather Rev.*, 122, 814–837, 1994.
- Mak, M., Dynamics of an atmospheric blocking as deduced from its local energetics, *Q. J. R. Meteorol. Soc.*, 117, 477–493, 1991.
- Mak, M. and Cai, M., Local barotropic instability, *J. Atmos. Sci.*, 46, 3289–3311, 1989.
- Mitchel et al., Climate change, Geneva, WMO, (WMO, 195/TP 100, Technical Note, 79), 1966.
- Mo, K. and Rasmusson, E. M., The 200 mb climatological vorticity budget during 1986–1989 as revealed by NMC analyses, *J. Clim.*, 6, 577–594, 1993.
- Murakami, M., Large-scale aspects of deep convective activity over the GATE area. *Mon. Weather Rev.*, 107, 994–1013, 1979.
- Nitta, T., A study of generation and conversion eddy available potential energy in the tropics, *J. Meteorol. Soc. Japan*, 45, 524–528, 1970.
- Nogués-Paegle, J. and Mo, K. C., Alternating wet and dry conditions over South America during summer, *Mon. Weather Rev.*, 125, 279–291, 1997.
- Pezzi, L. P., Rosa, M. B., and Batista, N. N. M., A corrente de jato subtropical sobre a América do Sul, *Climanálise Especial - Edição comemorativa de 10 anos. MCT/INPE/CPTEC*, 155–162, 1996.
- Rao, G. V. and Erdogan, S., The atmospheric heat source over the Bolivian plateau for a mean January, *Bound.-Layer Meteorol.*, 46, 13–33, 1989.
- Rao, V. B., Cavalcanti, I. F. A., and Hada, K., Annual variations of rainfall over Brazil and water vapour characteristics over South America, *J. Geophys. Res.*, 101, 26 539–26 551, 1996.
- Rao, V. B., Chapa, S. R., and Cavalcanti, I. F. A., Moisture budget in the tropics and the Walker circulation, *J. Geophys. Res.*, 103, 13 713–13 728, 1998.
- Rasmusson, E. M., Observational aspects of ENSO cycle teleconnections, eds: Glantz, M., Katz, R., and Nicholls, N., *Teleconnection linking worldwide climate anomalies*, Cambridge University Press, New York, 309–343, 1991.
- Sheng, J. and Hayashi, Y., Observed and simulated energy cycles in the frequency domain, *J. Atmos. Sci.*, 47, 1243–1254, 1990.
- Silva Dias, P. L., Schubert, W. H., and De Maria, M., Large-scale response of the tropical atmosphere to the transient convection, *J. Atmos. Sci.*, 115, 2689–2707, 1983.
- Smith, P. J., A note on energy conversions in open atmospheric systems, *J. Atmos. Sci.*, 27, 518–520, 1970.
- Trenberth, K. E. and Olson, J. G., An evaluation and intercomparison of global analysis from the National Meteorological Center and the European centre for Medium Range Weather Forecasts, *Bull. Am. Meteorol. Soc.*, 69, 1047–1057, 1988.
- Virji, H. A., A preliminary study of summertime tropospheric circulation patterns over South America estimated from winds, *Mon. Weather Rev.*, 109, 599–610, 1981.
- Wang, B. and Xie, X., A model for the boreal summer intraseasonal oscillation, *J. Atmos. Sci.*, 54, 72–86, 1997.